Journal of Zhejiang University SCIENCE A
ISSN 1673-565X (Print); ISSN 1862-1775 (Online)
www.zju.edu.cn/jzus; www.springerlink.com
E-mail: jzus@zju.edu.cn

Development of a non-cable whole tectorial membrane micro-robot for an endoscope*

Dong-dong YE†, Guo-zheng YAN†‡, Kun-dong WANG, Guan-ying MA
(*Department of Instrument, Shanghai Jiao Tong University, Shanghai 200240, China*)
†E-mail: yeddon@sjtu.edu.cn; gzhyan@sjtu.edu.cn
Received Nov. 23, 2007; revision accepted Feb. 20, 2008

Abstract: A novel non-cable whole tectorial membrane micro-robot for an endoscope is developed. The micro-robot we have fabricated and tested can propel itself in the intestine tract of a pig in an autonomous manner by earthworm-like locomotion. The silicone of bellow shape is laid over the outer surface of the micro-robot to reduce the affection of the viscoelastic properties of the intestine. Wireless power transfer and communication systems are employed to realize the non-cable locomotion of the micro-robot. The prototype of the micro-robot is 13.5 mm in diameter and 108 mm in length. The experimental results show that the towing force for the micro-robot is about 0.8 N, which is much smaller than the maximum driving force 2.55 N of the linear actuator. The supplying power of the wireless power transfer system fulfills the needs of the micro-robot system and the micro-robot can creep reliably in the large intestine of a pig and other contact environments.

Key words: Micro-robot, Endoscope, Intestine tract, Silicone of bellow shape, Linear actuator, Wireless power
doi:10.1631/jzus.A0720074 **Document code:** A **CLC number:** TP242.3

INTRODUCTION

Several methods exist for detecting the disease of the gastrointestinal (GI) tract. The traditional invasive endoscope tools easily damage the GI tissues because of their rigidity and are operated by doctors with difficulty and complication. A capsule endoscope is another way to investigate the GI tract, which can provide optical images of the whole small intestine painlessly without surgery (Mylonaki *et al*., 2003). However, this kind of endoscope suffers several limitations such as the limited energy supply of button batteries and passive forward mode. Therefore, various academic institutions and industries have embarked on the quest to improve the conventional and capsule GI endoscope.

Dario *et al*.(2002) presented an inchworm colonoscopic robot prototype. The former and latter sections alternately sucked the intestine tissue and one pneumatic extensor at its mid-section realized the locomotion. Phee *et al*.(2002a; 2003) proposed an endoscopic robot using corrugated pipe pneumatic actuators and *in vivo* experiments have been conducted validating the locomotion principle. Kim *et al.*(2005) fabricated a locomotive mechanism for an endoscopic capsule using two SMA (shape memory alloy) based springs. Some researchers proposed a legged endoscopic capsule employing the SMA as the miniaturized actuator (Menciassi *et al*., 2005a; 2005b; Gorini *et al*., 2006; Stefanini *et al*., 2006).

In all this literature, the pneumatic actuators have to trail an air pipe which is very difficult to bend to fit in with the intestinal tract. The SMA actuators have a minor temperature difference for deformation and reversion because of the low tolerance at high temperature of the intestinal tissues and have a lower locomotion speed. Besides, all the above endoscopes were powered by either a trailing cable or batteries. The former power supply style might highly influence the mobility of the micro-robot and injure the flimsy

‡ Corresponding author
* Project (No. 2007AA04Z234) supported by the Hi-Tech Research and Development Program (863) of China

living intestine tissue because of its rigidity and the latter cannot support the endoscopes for a long time. Finally, the viscoelastic properties of the intestine constantly mean the endoscopes have a lower locomotive efficiency.

In this paper, we present a novel non-cable whole tectorial membrane micro-robot prototype for the endoscope. It is composed of three linear actuators to simulate the squirm of the earthworm. The linear actuator employed the miniature DC motor (Kim *et al*., 2002) as the driving force, which has many advantages, such as a big driving force, small volume and easy control. The outer surface of the micro-robot is laid entirely over the silicone of bellow shape to reduce the influence of the viscoelastic properties of the intestine. Wireless modules are adopted for communication and power supply. The micro-robot is controlled by the VC-program running in the PC, starting by entering the intestine from the anus and can go forward and backward with different velocities.

LOCOMOTION PRINCIPLE

The earthworm can easily crawl into the ground and move in any environment. Its body is composed of many segments which elongate and contract to realize the creeping motion. The locomotion mode of the fabricated micro-robot simulates the squirm of the earthworm, which propels itself by single segment deformation and the difference of friction force between one mobile unit and the other immobile units.

Fig.1a shows the locomotion principle of the micro-robot. The micro-robot starts moving under the control signals as shown in Fig.1b. Status 1 is free elongation. At t_1, driver 3 is loaded on negative voltage, and then it contracts itself toward the left. The robot is in status 2 after driver 3 stops. At t_2, driver 3 is loaded on positive voltage and driver 2 is loaded on negative voltage, then driver 2 contracts itself toward the left. The robot is in status 3 after driver 2 stops. At t_3, driver 2 is loaded on positive voltage and driver 1 is loaded on negative voltage, and then driver 1 contracts itself toward the left. The robot is in status 4 after driver 1 stops. At t_4, driver 1 is loaded on positive voltage, and then the head cabin is propelled by driver 1 toward the left. The robot is in status 5 after driver 1 stops. Thus the robot finishes a pace forward. If the above action is repeated, the robot can move forward continuously. If the control signals are inversed, the robot will fall back.

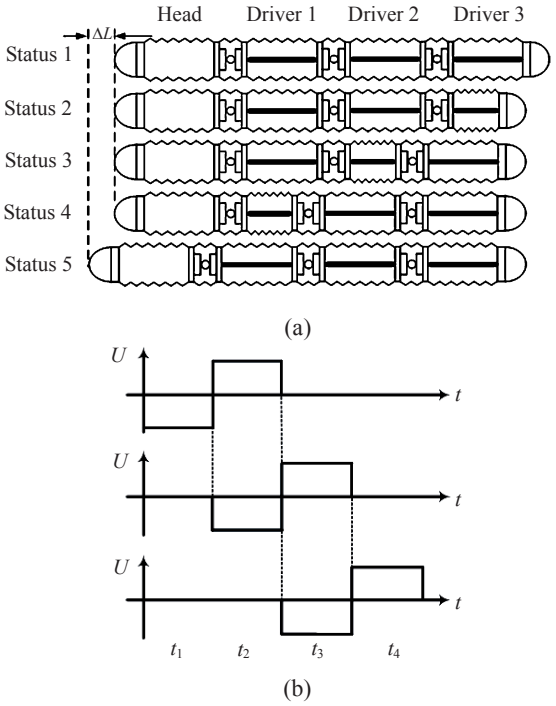

Fig.1 Scheme of the micro-robot locomotion principle (a) and control signal (b)

LINEAR ACTUATOR DESIGN

The linear actuator is an important part of the micro-robot because it plays a role in the contraction and extension of an earthworm muscle. The outer dimensions of the linear actuators are Φ10.3 mm×21 mm when contracted and Φ10.3 mm×29 mm in a stretched state as shown in Fig.2. The driving source based on a DC motor (Switzerland Maxon Co. Model: RE 6) is used for the linear actuators. The rotary speed of the DC motor is about 13 000 r/min with zero load. Therefore a reducer box will be fixed on the outer shell of the DC motor to slow down the output. Since the output of the reducer box is consecutive rotary motion, a nut and leading screw mechanism is adopted to accomplish the controllable rectilinear motion which ensures the deceleration while at the same time increasing force. When the nut slides forward and backward along the leading rails, the squirm movement of the micro-robot can be realized. The throw-over of the nut's motion direction depends on

the spacing tip. When the spacing tip is close-up, it can generate an electric single to the control module which can control the positive or inverted rotation of the DC motor.

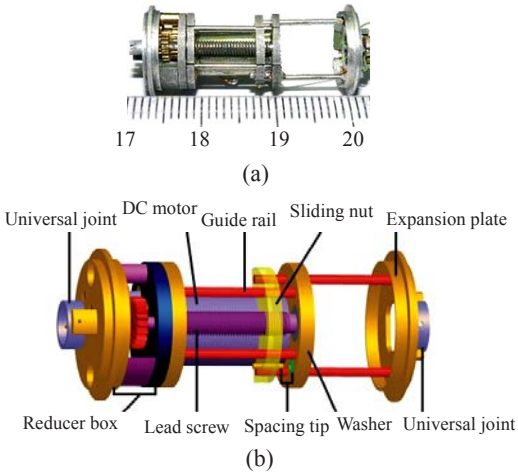

Fig.2 Scheme of the linear actuator in elongation state. (a) Prototype with full scale; (b) Pro/E design model

WHOLE TECTORIAL MEMBRANE DESIGN PRINCIPLE

Many paces were lost because of the deformation of the intestine tissue by friction force during elongation and retraction of the micro-robot. Therefore, studies relating to the efficiency of motion phases have been carried out based on the biomechanical and geometrical factors (Phee *et al*., 2002b; Dario *et al*., 2002).

According to our former work, the micro-robot can creep freely on the surface of the intestine when it has at least three units (Wang and Yan, 2007). However, the soft viscoelastic intestine wall will be stretched by the friction force and advances together with the micro-robot, as shown in Fig.3. After the largest advance L_c which is also the largest deformation of the intestine wall, the micro-robot continues to move forward to L which is the design step. If $L<L_c$, the micro-robot cannot move forward. Therefore, L_c is the critical stroke of the micro-robot and must be reduced to the minimum possible in order to improve locomotion efficiency. This paper supposes that f and μ are the sliding friction force and the coefficient between the micro-robot and the inner surface of the intestine wall, respectively. The mass of a driver unit is m. The contact part between the intestine wall and the micro-robot can be assumed to be a cylinder with the diameter D.

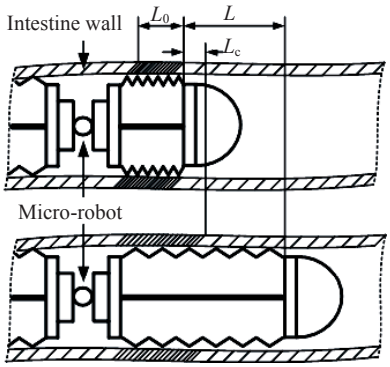

Fig.3 Scheme of intestine deformation and step loss of the micro-robot

According to the Cauchy-Euler meanings, the stress which leads to the deformation can be described as follows:

$$\sigma = \frac{f}{A} = \frac{mg\mu}{\pi Dh}, \tag{1}$$

where h is the thickness of the intestine wall.

If the length of the contact part between the intestine wall and the micro-robot is L_0 before elongation and is L_0+L_c after elongation, the strain ε can be described as follows:

$$\varepsilon = L_c / L_0. \tag{2}$$

The intestine is a kind of biological material and has its own fixed mechanical constitutive relation. According to the well-known pseudo-elastic constitutive equation $\sigma=\gamma\varepsilon^2$ (Fung, 1990; Phee *et al*., 2003), the following equation can be deduced:

$$L_c = \sqrt{\frac{mg\mu L_0^2}{\pi Dh\gamma}}, \tag{3}$$

where γ=12.25±3.675 kPa for longitudinal strips of the intestine tissue, which can be calculated from (Gregersen, 2006).

As the micro-robot is manufactured, the mass

and diameter of the driver are determined. In order to reduce the effectual magnitude of L_0, the surface of the micro-robot can be made in a bellow shape. In addition, the bending resistance of a bellow shape is higher than that of a plane shape. Therefore, L_c is a monotonically rising function of μ, as shown in Fig.4. Here, L_0=18 mm when the surface of the micro-robot is a plane shape and L_0=8 mm when a bellow shape. It can be found that L_c has an obvious decline when L_0 changes from 18 mm to 8 mm.

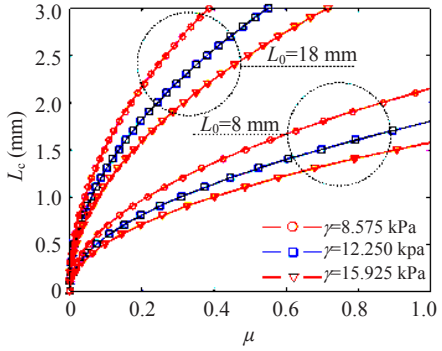

Fig.4 Relationship between the largest advance L_c and the friction coefficient μ when the length of the contact part between the intestine wall and the micro-robot is 18 mm and 8 mm, respectively

Since the micro-robot will be laid over a membrane to protect itself from water penetration, a material with a low friction coefficient should be selected first (Fig.4). According to (Li *et al*., 2006), silicone has the ability of self-lubricity and the friction coefficient with the intestine wall is lower than 0.1. Besides, the silicone has a wide working temperature range from −100 °C to +350 °C and excellent electro-insulating properties, is physiologically inert and has good mildew resistance, which absolutely satisfies the particular conditions of the inner intestine tract. Therefore, a silicone of bellow shape is selected as the surface of the micro-robot.

WIRELESS POWER TRANSFER SYSTEM

In order to ensure the locomotion stabilization and validity of the micro-robot in the special conditions of the intestine tract, a stable and enduring power supply is essential. Some of the literature has validated the feasibility of wireless power transfer for remotely located micro-systems using inductive coupling (Heetderks, 1988; Kopparthi and Ajmera, 2004; Son *et al*., 2005).

This power transfer style needs two coils. One is the launching coil and the other is the receiving coil. The launching coil, which is a solenoid, will surround the patient's trunk and has an inductive link with the receiving coil, embedded in the head cabin of the micro-robot. The launching coil is driven by a class E amplifier or a switching circuit. A parallel resonant circuit (PRC) is employed on the receiving coil. The inductive links can be generalized as a lumped transfer model, as shown in Fig.5. C_2 is the parallel resonant capacitor. R_1 and R_2 are the respective series-resistances of L_1 and L_2. R_L is the resistor which is used to simulate the load. C_1 is the series-resonant capacitor to drive a sinusoidal high-amplitude electric current $\tilde{I}_1$.

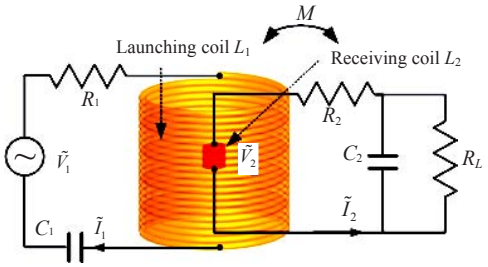

Fig.5 Transfer model and equivalent circuit

The maximum coupling efficiency can be achieved when the launching and receiving circuits are of tuned resonance. The resonance frequency is calculated as follows:

$$\omega=\frac{1}{\sqrt{l_1C_1}}=\frac{1}{\sqrt{l_2C_2}}, \tag{4}$$

where l_1 and l_2 are the self-inductances of the two coils.

The maximum achievable link efficiency with secondary resonance is expressed as (Ma *et al*., 2007)

$$\eta_{\max}=\frac{K^2\omega^2l_1l_2}{4R_1R_2}, \tag{5}$$

where K is the coupling coefficient.

The power transfer link can be optimized according to Eq.(5). In this paper, the launching coil was constructed with a single-layer structure, 400 mm in outside diameter, 360 mm in inner diameter, 260 mm

in length and 120 turns of AWG 16 solid copper wire. The receiving windings were round on an ABS (acrylonitrile butadiene styrene) skeleton with I-shaped cross-section and 7.6 mm aperture size. This small coil was 11.5 mm in outer diameter, 8 mm in inner diameter, 10 mm in length, and a multilayer structure of a total 315 turns of AWG 35 wire. A ferrite core could be inserted into or removed from the receiving coil skeleton. The receiving coil will be integrated with a commutation and voltage-stabilizing electric circuit, and the output of the electric circuit will supply the micro-robot with stable voltage.

COMMUNICATION AND CONTROL SYSTEM

Most studies have proved that there is electromagnetic power absorption in biotic tissue and the radiation efficiency will change with a different location of the radiation source (Kuster and Balzano, 1992; Pandit *et al*., 1996; Repacholi, 1998). In order to minimize this defect, we established a modeling of the electromagnetic power absorption of the radiation source in biotic tissue through which the simulation experiment was studied, and obtained an optimum frequency range from 100 MHz to 1 GHz. There are two frequency bands of 433 MHz and 915 MHz (industrial, scientific and medical) in this range. The former band is used as the carrier frequency in our system because of its lower electromagnetic power absorption value, which meets the ICNIRP (International Commission on Non-Ionizing Radiation Protection) Guidelines (Valdastri *et al*., 2004).

The chip nRF 905, product of NORDIC, is selected as the wireless transceiver, which can automatically handle preamble and CRC (cyclic redundancy check). The single chip adopts the GFSK (Gauss frequency shift key) modulation schemes because of its low power consumption and high anti-jamming ability. The assembled remote wireless communication module is composed of transceiver chip, MCU (Silicon Laboratories in Texas, Model: C8051F330) and antenna module. A special small whip antenna was used for the miniature transceiver, 12 mm in length and 0.25 mm in diameter, because of the space restriction of the micro-robot.

Fig.6 shows the block diagram of the communication and control system of the micro-robot endoscope. The control parameters are transmitted by RS 232 transceiver from the PC to the local wireless communication module, which includes MCU and the counterpart of the RF (radio frequency) communication link. The RF communication chip broadcasts the parameters to the remote wireless communication module embedded in the head cabin of the micro-robot (Fig.7). The maximum transfer bit rate is up to 50 kbps, which is sufficient for most applications. Therefore, the local and remote wireless communication modules combine into a low power, two-channel and bidirectional wireless communication system.

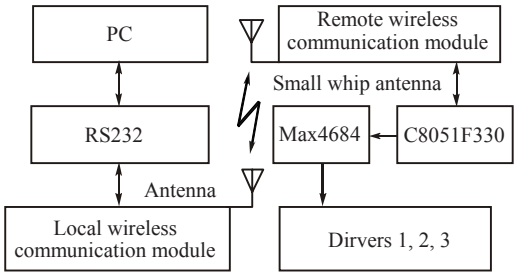

Fig.6 Communication and control functional block diagram of the micro-robot

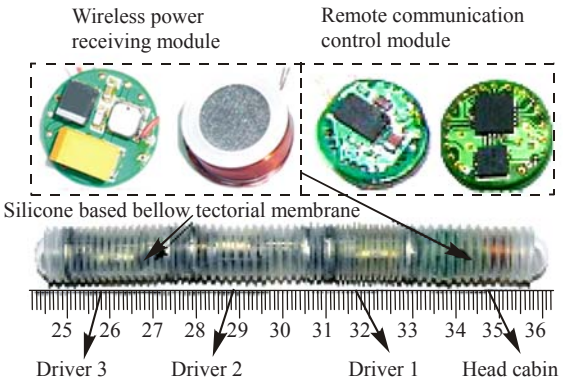

Fig.7 Photograph of the non-cable whole tectorial membrane micro-robot prototype

The parameters received by the micro-robot are decoded by C8051F330 to generate a certain sequence waveform as shown in Fig.1b. The chip of C8051F330 is suitable for fabricating the earthworm-like micro-robot because of a precision programmable 25 MHz internal oscillator with a dimension of 4 mm×4 mm in area. The analog switch (Max4684) is employed for switching the current of the linear actuator. The waveform signals amplified

and loaded on the linear actuators can control the direction of motion, speed and towing force.

MICRO-ROBOT FABRICATION AND EXPERIMENTS

The micro-robot prototype (108 mm in length and 13.5 mm in diameter) is composed of a head cabin, three actuators and a silicone of bellow shape tectorial membrane, as shown in Fig.7. The wireless power receiving module and remote communication control module are installed in the head cabin. Three gimbal joints connect four parts of the micro-robot to ensure that the robot can adjust its poses in the complex environment of the intestine. The weight is 16.1 g and the design pace is 8 mm.

The silicone of bellow shape is an elastic body and will apply force on the linear actuator during the movement of the micro-robot. Therefore, we fix one of its ends on the experiment table and apply a varied magnitude of force on the other end using an analog push-pull gauge (SUNDOO Instruments Co., Model: SN-10). At the same time, the corresponding deforming displacement L is measured. As shown in Fig.8, the approximate linear relationship between L and the elastic force F_e can be distributed in three parts: 26.0~16.7 mm, 16.7~14.4 mm and 14.4~12.4 mm.

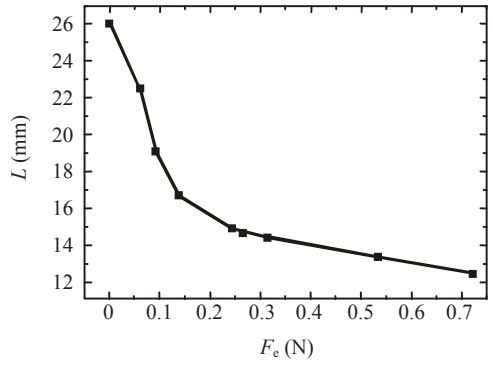

Fig.8 Relationship between the displacement L and the elastic force F_e

In this paper, the silicone of bellow shape works in the first part (26.0~16.7 mm) of Fig.8 because the design pace of the linear actuator is 8 mm. Then the linear actuator is covered by the bellow and the driving force is measured at a different load from 0.5 N to 2.6 N, as shown in Fig.9. Obviously the driving force F has an approximately linear relationship with the driving current I and the maximum driving force of the linear actuator is about 2.55 N, which fulfills the locomotion needs of the micro-robot. Here the working rated voltage is 3 V.

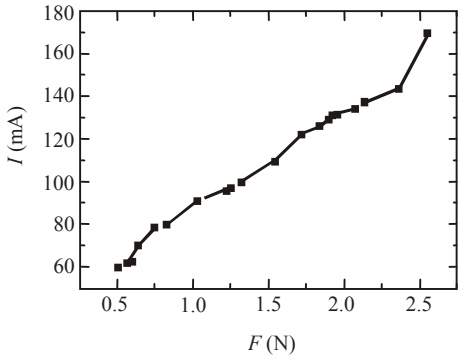

Fig.9 Relationship between the driving force F and the driving current I

Then the wireless power receiving coil with load R_L is placed in the middle of the launching coil. Fig.10 shows the three curves between the measured input power E_{in} and output current I_{out}. The deflected degrees of the axial direction of the receiving and launching coil are 0°, 25° and 50°, respectively. In the experiment, the launching power is adjusted from 0 to 17.4 W and the load R_L is about 220 Ω. The transmission frequency was kept at 36.9 kHz.

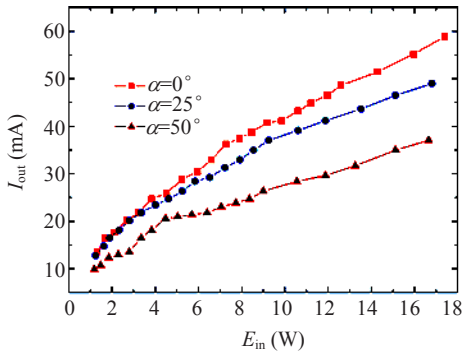

Fig.10 Wireless power transfer experiment on axial separation between two coils

For testing the locomotion ability of the micro-robot, we carried out an *in vitro* experiment at room temperature for simulating the actual locomotion surroundings, as shown in Fig.11.

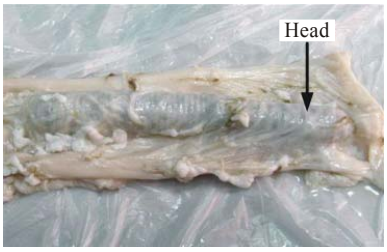

Fig.11 Photograph of the micro-robot in a large intestine *in vitro* experiment

Fig.12 shows the measured locomotion according to different contact environments. The theoretical speed of the micro-robot is approximately 1.95 mm/s. Then, a segment of smooth rubber pipe with a length of 67 cm is spread out on the experimental bench. Firstly, the micro-robot is guided into one end of the rubber pipe, which is 14.5 mm in diameter, and has no collapse. The micro-robot starts creeping toward the other end of the rubber in 8.5 min. Therefore the speed of the micro-robot is about 1.31 mm/s on the surface of the rubber pipe. After that, a segment of fresh large intestine of a pig with the same length of 67 cm, which has been washed off the stool, is spread out on the experimental bench. Repeating the above-mentioned experimental procedures, the speed in the large intestine of pig is measured at about 1.01 mm/s.

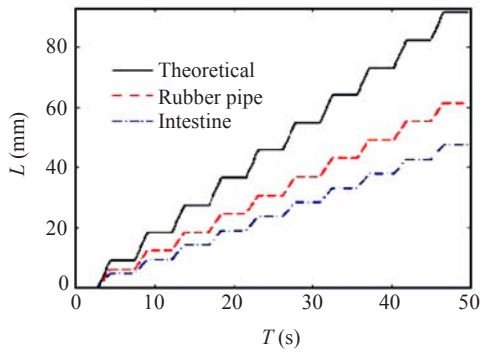

Fig.12 Result of micro-robot locomotion performance

DISCUSSION

The accordion-like motion of the bellow is simulating the locomotion style of the earthworm, which has proven to be an effective way of reducing adhesion. Since the bellow works within its first mechanical range according to Fig.8, the elastic force will not exceed 0.12 N which can be easily compressed by the linear actuator. When the linear actuator elongates, the bellow will push the expansion plate of the linear actuator back, depending on its elastic restitution. In addition, the maximum dissipative power of the linear actuators is nearly 540 mW when its output force is 2.55 N, as shown in Fig.9. However, it can be easily found from the *in vitro* experiment that the dissipative power of a linear actuator is actually close to 230 mW. Then, the towing force for the micro-robot will be less than 0.8 N.

Since the micro-robot adopts wireless power transfer and communication, the endoscope really realizes a non-cable style, which reduces the friction force brought by the trailing cable in a traditional micro-robot endoscope system. From Fig.10, the wireless power transfer system can supply the micro-robot with different currents according to different launching power. It can also be found that the launching current and voltage are 1.16 A and 15 V, respectively, when the maximum receiving power is 841.5 mW. The maximum dissipative power of the micro-robot in the large intestine *in vitro* experiment is only about 500 mW when two linear actuators work simultaneously, as shown in Fig.1a. Under such conditions, the launching current and voltage are about 1.03 A and 11.3 V, respectively. Then the launching power will be fixed and the receiving coil will supply the micro-robot with enough stable power through the commutation and voltage-stabilizing electric circuit. Moreover, according to (Lenaerts and Puers, 2007), the electromagnetic field required for wireless power transfer will not exceed the ICNIRP standards for safety. However, the transfer efficiency declines with the augmentation of the deflected degrees of the axial direction of the receiving and launching coil. The transfer efficiency was close to 0 when the axial direction of the receiving coil was perpendicular to the axial direction of the launching coil. Employing multi-launching coils or adopting a 3D receiving coil may relieve this issue (Lenaerts and Puers, 2007). Related experiments are being conducted.

In previous experiments, the micro-robot has a good ability to navigate in a rigid tube which does not translate to good navigation in the intestine tract, as the viscoelastic properties differ greatly to those in rigid tubes. In this paper, the silicone of bellow shape tectorial membrane is applied to the micro-robot. The

bellow shape surface and low friction coefficient reduce the influence of the viscoelastic properties and promote locomotion efficiency. Moreover, the height of the ripple is only 1.4 mm and the tissue of the intestine is not found to get into the troughs of the bellow to cut down the locomotion efficiency, as shown in Fig.11. However, it also can be found from Fig.12 that the locomotion speed in the large intestine of a pig is still far less than the theoretical speed and even lower than that in the rubber pipe where the micro-robot has little pace loss. The reason may be the collapse of the intestine and the lack of clamping mechanisms. We have been researching a clamping mechanism which installs two supporting gas bags on the ends of the robot. Thus a micro-pump which can be used in the inner intestine is in development. Certainly there will be navigational equipment based on vision, which also can supply clear images of the inner intestine for clinical diagnosis, integrated in the front end of the next endoscopic micro-robot, to fit in with the loops of the large intestine such as alpha and gamma loops (Wang *et al*., 2006).

CONCLUSION

In this paper we designed and fabricated a novel non-cable whole tectorial membrane micro-robot system for an endoscope. The system adopts the earthworm-like micro-robot based on a new linear actuator. The linear actuator is covered by a silicone of bellow shape. This whole tectorial membrane micro-robot is more suitable for examining the condition of the intestine tract. The communication and power supply are all wireless in the proposed system, which is different from the conventional robot with trailing cable and can reduce the resisting force coming from the trailing cable and is more suitable for locomotion in a narrow and rough environment such as the human intestine. Experimental results show that the fabricated micro-robot can move reliably in the large intestine of a pig with a velocity of 1.01 mm/s. This research further promotes the availability, reliability and security of locomotion in the intestine tract of the endoscopic micro-robot.

References

Dario, P., Ciarletta, P., Menciassim, A., Kim, B., 2002. Modelling and Experimental Validation of the Locomotion of Endoscopic Robots in the Colon. ISER 02 Int. Symp. on Experimental Engineering, Santangelo, Italy, p.445-453.

Fung, Y.C., 1990. Biomechanics: Motion, Flow, Stress and Growth. Springer-Verlag, New York, p.353-447.

Gorini, S., Quirini, M., Menciassi, A., Permorio, G., Stefanini, C., Dario, P., 2006. A Novel SMA-based Actuator for a Legged Endoscopic Capsule. First IEEE/RAS-EMBS Int. Conf. on Biomedical Robotics and Biomechatronics, Pisa, Italy, p.443-449. [doi:10.1109/BIOROB.2006.1639128]

Gregersen, H., 2006. Biomechanics of the Gastrointestinal Tract. People's Medical Publishing House, Beijing, China, p.216-236 (in Chinese).

Heetderks, W.J., 1988. RF powering of millimeter- and submillimeter-sized neural prosthetic implants. *IEEE Trans. on Biomed. Eng.*, **35**(5):323-327. [doi:10.1109/10.1388]

Kim, B., Lim, H.Y., Kim, K.D., Jeong, Y.K., Park, J.O., 2002. A Locomotive Mechanism for a Robotic Colonoscopy. IEEE/RSJ Int. Conf. on Intelligent Robots and System IROS-02, Lausanne, Switzerland, p.1373-1378. [doi:10.1109/IRDS.2002.1043946]

Kim, B., Lee, S., Park, J.H., Park, J.O., 2005. Design and fabrication of a locomotive mechanism for capsule-type endoscopes using shape memory alloys. *IEEE/ASME Trans. on Mechatron.*, **10**(1):77-86. [doi:110.1109/TMECH.2004.842222]

Kopparthi, S., Ajmera, P.K., 2004. Power Delivery for Remotely Located Microsystems. IEEE Region 5 Conf.: Annual Technical and Leadership Workshop, Norman, USA, p.31-39. [doi:10.1109/REG5.2004.1300156]

Kuster, N., Balzano, Q., 1992. Energy absorption mechanism by biological bodies in the near field of dipole antennas above 300 MHz. *IEEE Trans. on Vehic. Technol.*, **41**(1):17-23. [doi:10.1109/25.120141]

Lenaerts, B., Puers, R., 2007. An inductive power link for a wireless endoscope. *Biosens. Bioelectron.*, **22**(7):1390-1395. [doi:10.1016/j.bios.2006.06.015]

Li, J., Huang, P., Luo, H.D., 2006. Experimental study on friction of micro machines sliding in animal intestines. *Lubric. Eng.*, **3**:119-122 (in Chinese).

Ma, G.Y., Yan, G.Z., He, X., 2007. Power transmission for gastrointestinal microsystems using inductive coupling. *Physiol. Meas.*, **28**(3):9-18. [doi:10.1088/0967-3334/28/3/N01]

Menciassi, A., Moglia, A., Gorini, S., Permorio, G., Stefanini, C., Dario, P., 2005a. Shape memory alloy clamping devices of a capsule for monitoring tasks in the gastrointestinal tract. *J. Micromech. Microeng.*, **15**(11):2045-2055. [doi:10.1088/0960-1317/15/11/008]

Menciassi, A., Gorini, S., Moglia, A., Pernorio, G., Stefanini, C., Dario, P., 2005b. Clamping Tools of a Capsule for

Monitoring the Gastrointestinal Tract. Proc. IEEE Int. Conf. on Robotics and Automation, Barcelona, Spain, p.1309-1314. [doi:10.1109/ROBOT.2005.1570296]

Mylonaki, M., Fritscher-Ravens, A., Swain, P., 2003. Wireless capsule endoscopy: a comparison with push enteroscopy in patients with gastroscopy and colonoscopy negative gastrointestinal bleeding. *Gut*, **52**(8):1122-1126. [doi:10.1136/gut.52.8.1122]

Pandit, V., McDermott, R., Lazzi, G., Furse, C., Gandhi, O., 1996. Electrical Energy Absorption in the Human Head from a Cellular Telephone. IEEE Visualization Proc., San Francisco, USA, p.371-374.

Phee, L., Menciassi, A., Gorini, S., Pernorio, G., Arena, A., Dario, P., 2002a. An Innovative Locomotion Principle for Mini Robots Moving in the Gastrointestinal Tract. IEEE Int. Conf. on Robotics and Automation, Washington DC, USA, **2**:1125-1130. [doi:10.1109/ROBOT. 2002.1014694]

Phee, L., Accoto, D., Menciassi, A., Stefanini, C., Carrozza, M.C., Dario, P., 2002b. Analysis and development of locomotion devices for the gastrointestinal tract. *IEEE Trans. on Biomed. Eng.*, **49**(6):613-616. [doi:10.1109/TBME.2002.1001976]

Phee, L., Menciassi, A., Accoto, D., Stefanini, C., Dario, P., 2003. Analysis of robotic locomotion devices for the gastrointestinal tract. *Rob. Res.*, **6**:467-483. [doi:10.1007/3-540-36460-9_31]

Repacholi, M.H., 1998. Low-level exposure to radiofrequency electromagnetica fields: health effects and research needs. *Bioelectromagnetics*, **19**:1-19. [doi:10.1002/(SICI)1521-186X(1998)19:1<1::AID-BEM1>3.3.CO;2-8]

Son, J.H., Hwang, J.S., Songa, K.M., Ryub, M.H., Kima, J.D., Baanga, S., 2005. Design of Millimeter-sized Coils for Power Transmission to *in vivo* Robotic Capsules. Proc. 3rd IASTED Int. Conf. on Biomedical Engineering, Innsbruck, Austria, p.499-502.

Stefanini, C., Menciassi, A., Dario, P., 2006. Modeling and experiments on a legged microrobot locomoting in a tubular, compliant and slippery environment. *Int. J. Rob. Res.*, **25**(5-6):551-560. [doi:10.1177/0278364906065876]

Valdastri, P., Menciassi, A., Arena, A., Caccamo, C., Dario, P., 2004. An implantable telemetry platform system for *in vivo* monitoring of physiological parameters. *IEEE Trans. on Inf. Technol. Biomed.*, **8**(3):271-278. [doi:10.1109/TITB.2004.834389]

Wang, K.D., Yan, G.Z., 2007. Micro robot prototype for colonoscopy and *in vitro* experiments. *J. Med. Eng. Technol.*, **31**(1):24-28. [doi:10.1080/03091900500233759]

Wang, K.D., Yan, G.Z., Zuo, J.Y., 2006. Active micro robot colonoscopy's navigation based on vision. *High Technol. Lett.*, **16**(4):372-376.